

Electrical Properties in Large Frequency and Temperature Ranges of $\text{Sr}_{0.6}\text{Ca}_{0.4}\text{TiO}_3$ Ceramics

H. Ait Laasri^{a,b}, A. Tachafine^a, D. Fasquelle^a, N. Tentillier^a,
M. Elaamani^b, L. C. Costa^c and J. -C. Carru^a

^a *Unité de Dynamique et Structure des Matériaux Moléculaires, Université du Littoral - Côte d'Opale, 50 rue Ferdinand Buisson, 62228 Calais, France.*

^b *Unité de Dynamique et Structure des Matériaux Moléculaires, Université du Littoral - Côte d'Opale, 50 rue Ferdinand Buisson, 62228 Calais, France.*

^c *I3N and Physics Department, University of Aveiro, Campus Universitário de Santiago 3810-193 Aveiro, Portugal.*

Doi : <https://doi.org/10.47011/13.3.3>

Received on: 08/08/2019;

Accepted on: 12/12/2019

Abstract: Lead-free $\text{Sr}_{0.6}\text{Ca}_{0.4}\text{TiO}_3$ (SCT) ceramic was prepared by the solid state reaction route. X-Ray diffraction technique showed the phase purity and identified the orthorhombic perovskite structure of the material. Scanning Electronic Microscopy observation evidenced homogeneous morphology and dense microstructure for the ceramic. The dielectric and conductivity properties of the sample were studied using complex impedance measurement technique in a wide range of frequencies and temperatures: from 100 Hz to 1.8 GHz and from 25°C to 550°C. The ceramic exhibits a stable dielectric permittivity and low dielectric losses in frequency and temperature up to 200°C. This is very interesting in view of developing high-quality lead-free ceramic capacitors for applications requiring high temperatures; for example, in cars. The increase in dielectric permittivity for temperatures higher than 200°C may be related to oxygen vacancies that are heat-activated in the material. Dielectric losses show the existence of a dielectric relaxation at low temperatures and low frequencies. Conductivity measurement investigated at high temperatures show on one hand high AC conductivity values attributed to the high temperature jumping process and on the other hand two electrical conductivity mechanisms above 400° C in the material.

Keywords: Strontium calcium titanate, Ceramic, Structure, Dielectric properties, Conductivity.

Introduction

Due to the multiplication of standards and norms of telecommunication systems and in the era of miniaturization, an important need for frequency tunable components and multifunctional devices appears [1-4]. Many solutions can be considered, among which is the introduction of new materials and/or new structures able to modify the properties of the

devices constituted thereof. In order to do so, we must use materials presenting low losses and high dielectric permittivity stable in frequency and temperature [5]. Most electronic components contain lead-based materials, because of their interesting electric and ferroelectric properties. Among them are pure PbTiO_3 or doped $(\text{Pb,Zr})\text{TiO}_3$ [6-7]. For environmental reasons, as

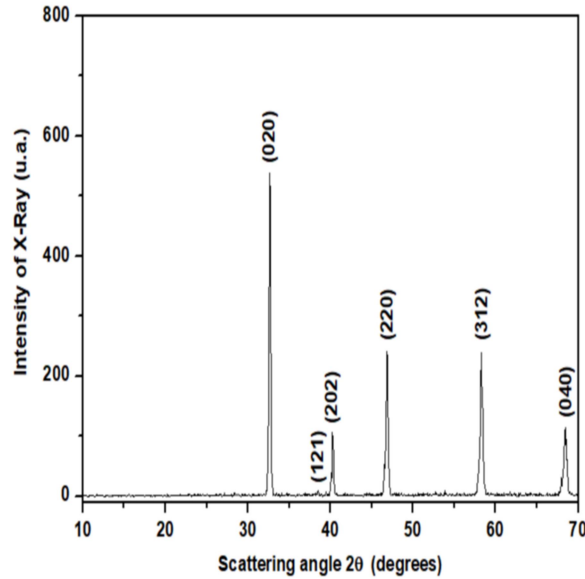
evidenced by the legislation passed by the European Union in this effect [8-9], all research turned toward the environment-friendly materials. It is now necessary to replace Pb-based materials with lead-free materials [10]. Barium titanate (BaTiO_3) material has good dielectric properties which make it the most used base material to elaborate high dielectric permittivity capacitors [11]. However, the variations of its dielectric permittivity with temperature are too important for practical applications [12]. The strontium titanate (SrTiO_3), which is another simple perovskite ABO_3 ferroelectric material, displays a paraelectric behavior with cubic symmetry at room temperature [13]. Additionally, this material presents high dielectric permittivity and low dielectric losses at high frequency [14], which gives advantages for electrical applications. To improve the electrical properties of SrTiO_3 ceramics, it is possible to substitute A-sites with another divalent cation, such as Ba^{2+} , Mg^{2+} , Ce^{2+} or Ca^{2+} [15-20]. In particular, the $\text{Sr}_{1-x}\text{Ca}_x\text{TiO}_3$ solid solution undergoes phase transition and exhibits different structures and behaviors, depending on the composition of calcium. It shows a ferroelectric behavior for the composition range $0.0018 < x \leq 0.016$, a relaxor one for $0.016 < x \leq 0.12$ and an anti-ferroelectric one for $0.12 < x \leq 0.4$ such as for example around 185 K for $x=0.25$ [21-22]. Recent studies conducted at low frequencies have shown that it is possible to increase the dielectric constant value of the SrTiO_3 ceramic by doping with low calcium rates from 2% to 4% [23] or decreasing it for rates higher than 12% [24]. In the present work, we report on the structural and dielectric properties of strontium calcium titanate ($\text{Sr}_{1-x}\text{Ca}_x\text{TiO}_3$) ceramics in which strontium is substituted by a high rate of calcium, which is 40% to obtain lead-free ferroelectric materials with improved properties for electronic radiofrequencies and microwave applications. In fact, the lowest losses have been measured on high rates of calcium [25-26]. We have studied this bulk material both at room temperature in a large frequency range from 100 Hz to 1.8 GHz and in a large temperature range from room temperature to 510°C to evaluate its possible use in high-temperature and/or high-frequency environments. The measurement of complex impedance spectroscopy was used for dielectric characterization.

Experimental

Ceramic samples with 3 mm of diameter and 3 mm of thickness were prepared by the conventional solid-state reaction method. $\text{Sr}_{0.6}\text{Ca}_{0.4}\text{TiO}_3$ samples (SCT) were prepared using stoichiometric proportions of high-purity powders of strontium carbonate (SrCO_3) (Fluka, 98%), calcium carbonate (CaCO_3) (Fluka, 98%), and titanium oxide (TiO_2) (Prolabo, 99%). Appropriate quantities of these precursors were then weighed, thoroughly mixed and pestled in an agate mortar and subsequently calcined at 1250°C in alumina crucibles under an air atmosphere for 15 hours. After cooling, the obtained powder was ground and then pressed under a load of 0.5 ton into pellets of 3-mm diameter and 3-mm thickness. The pellets were subsequently sintered at 1400°C for 5 hours in air. X-ray diffraction (XRD) analysis was performed at room temperature on the powdered samples, in a Philips X'PERT system, with a $K\alpha$ radiation ($\lambda=1.54056 \text{ \AA}$) at 40 kV and 30 mA, with a step of 0.05° and a time per step of 1 second. Microstructures were examined by Scanning Electronic Microscopy (SEM). Silver-paint electrodes were deposited on the samples for electrical measurements. Temperature and frequency dependences of the dielectric permittivity and loss-tangent of the ceramics were investigated from 80 K to 800 K and from 20 Hz to 1 MHz using an Agilent 4284A LCR meter.

Results and Discussion

Fig. 1 shows the XRD patterns of the SCT powder at room temperature. All the peaks of the XRD diagrams were indexed to the pure perovskite phase. The peaks are intense and very narrow, showing good crystallinity of the samples. No peaks were detected which could be assigned to secondary phases or unreacted oxides. The observed peaks are characteristic of an orthorhombic structure [22] according to International Center Diffraction Data (ICDD) files Ref. 01-089-8032. The lattice parameters are calculated using the unit-cell refinement software Celref [27]. The (a, b, c) dimensions and unit cell volume values are respectively: 5.4960 \AA , 5.4881 \AA , 7.7418 \AA and 233.51 \AA^3 . The average crystallite size calculated by the Scherrer's Eq. (1) is about 42 nm.

FIG. 1. XRD patterns of Sr_{0.6}Ca_{0.4}TiO₃ powders.

$$D = \frac{k\lambda}{\beta \cos \theta} ; \text{ where:} \quad (1)$$

β : Peak width at half maximum height (FWHM) (rad);

θ : Bragg diffraction angle;

λ : X-ray wavelength (1.5406 Å);

k : Dimensionless shape factor (0.9).

Fig. 2 shows the SEM microphotograph of the SCT ceramic. The microphotograph shows a homogeneous microstructure and well-developed grain morphologies. The average grain size is estimated using the MagniSci software and is about 2 μm which is about 45 times the average crystallite size. The average grain boundary size is about 0.05 μm . The compactness of the SCT ceramic is about 93%.

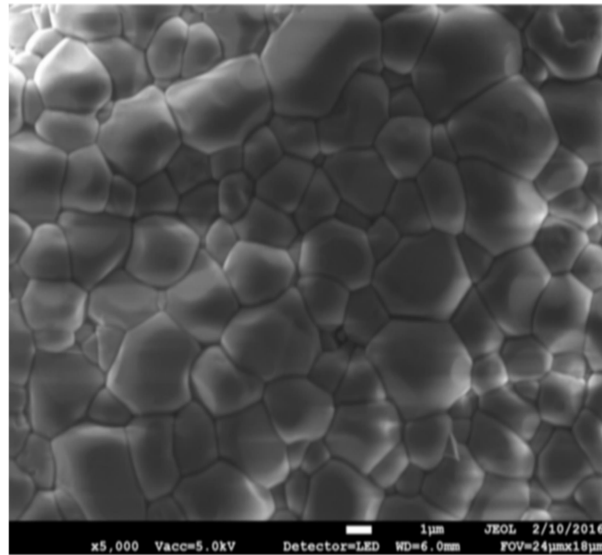
FIG. 2. SEM microphotograph of the Sr_{0.6}Ca_{0.4}TiO₃ ceramic.

Fig. 3 presents the frequency dependence of the dielectric permittivity ϵ' of SCT ceramic from 100 Hz to 1 GHz at room temperature. The dielectric permittivity shows a good stability all over the frequency range ($\epsilon' \approx 200$). This is an advantage for high-frequency components. This

ϵ' value is lower than that reported for low calcium rates ($x = 0.02$ and $\epsilon' \approx 310$) [23]. In fact, doping with Ca rates higher than 12% decreases the dielectric permittivity value, as shown in recent studies [24].

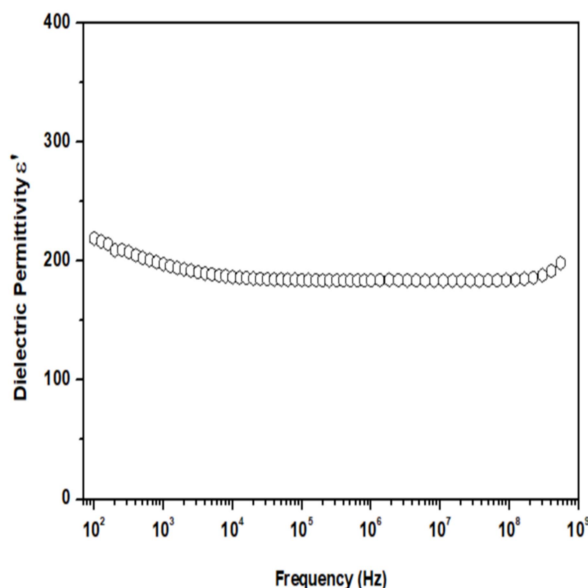


FIG. 3. Dielectric permittivity (ϵ') of the $\text{Sr}_{0.6}\text{Ca}_{0.4}\text{TiO}_3$ ceramic in frequency at room temperature.

The frequency dependence of the dielectric loss tangent ($\text{tg}\delta$) of SCT ceramic from 100 Hz to 1 GHz at room temperature is shown in Fig. 4. The dielectric loss tangent decreases from 100 Hz to 1 MHz down to $3 \cdot 10^{-4}$ due to space-charge polarization losses and increases from 10 MHz to 1 GHz up to $6 \cdot 10^{-2}$ due to intrinsic losses [28]. These $\text{tg}\delta$ values are of interest for

radiofrequency and microwave applications, especially as the dielectric permittivity of the ceramic is stable over the whole frequency range. It was not possible to collect accurate data from 1 MHz to 12 MHz, because the pellet resistance was too high and definitely out of the measurement range for the HP4291A.

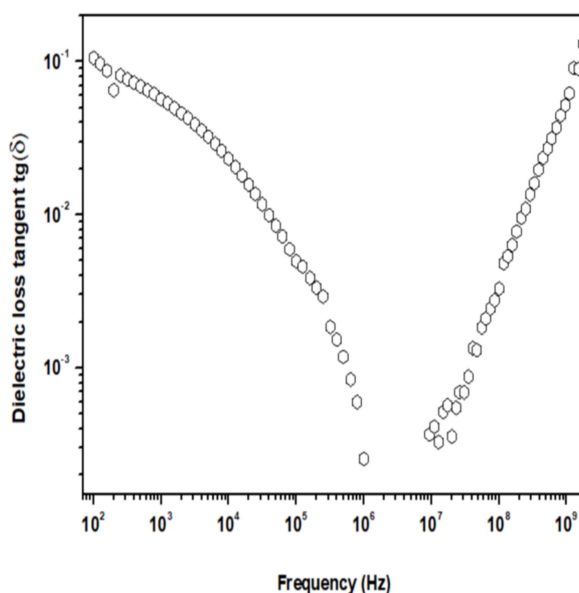


FIG. 4. Dielectric loss tangent ($\text{tg}\delta$) of the $\text{Sr}_{0.6}\text{Ca}_{0.4}\text{TiO}_3$ ceramic in frequency at room temperature.

Fig. 5 shows the temperature dependence of the dielectric permittivity of SCT ceramic from room temperature to 510°C at different frequencies from 100 Hz to 1 MHz. The dielectric permittivity is constant ($\epsilon' = 200$) in temperature up to 200°C for all the frequencies

and no phase transition is observed. This stability of the dielectric permittivity in frequency and temperature up to 200°C is very interesting and shows that SCT could be used in ceramic capacitors applied to high-temperature environments, such as the automotive or military

field for example [29]. The dielectric permittivity is stable over a temperature range which is all the more so as the frequency increases. Indeed, it is almost stable from room temperature to about 300°C for $f = 1$ kHz, to about 375°C for $f = 10$ kHz and above 500°C for $f = 1$ MHz. For each temperature, there is therefore a threshold frequency F_T , since at this frequency, the dielectric permittivity starts to rise at this temperature. It can be noted that above 450°C , a peak can be seen clearly for example at

1 GHz and about 500°C with $\epsilon' \approx 4000$. Its origin may be a relaxation, but more probably an extrinsic effect of Maxwell-Wagner interfacial polarization between the grains (semiconductors) and the grain boundaries (electrical insulators). The maximal amplitude of the peak decreases as the measurement frequency increases. At a given ϵ' , for example 1000 , it is observed that the frequency increases as the temperature increases, which means that the Maxwell-Wagner polarization is thermally activated [30].

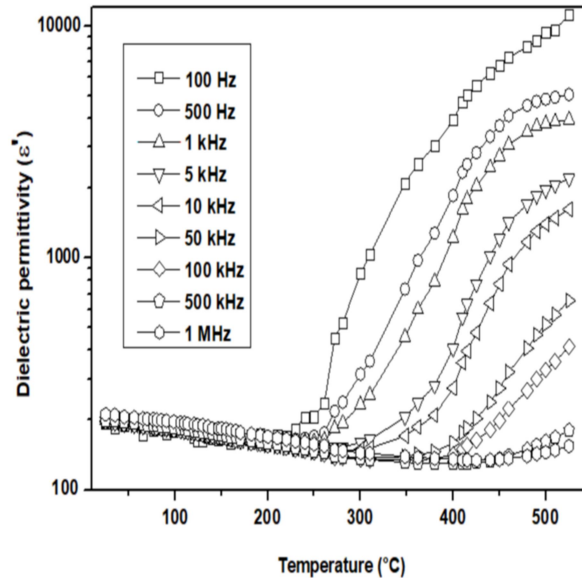


FIG. 5. Dielectric permittivity (ϵ') of the $\text{Sr}_{0.6}\text{Ca}_{0.4}\text{TiO}_3$ ceramic in frequency and temperature.

The temperature dependence of the threshold frequency is shown in Fig. 6. The threshold frequency increases with increasing temperature. The calculated activation energy (1.74 eV)

shows that the increase in dielectric permittivity with temperature may be related to oxygen vacancies that are heat-activated in the material [31].

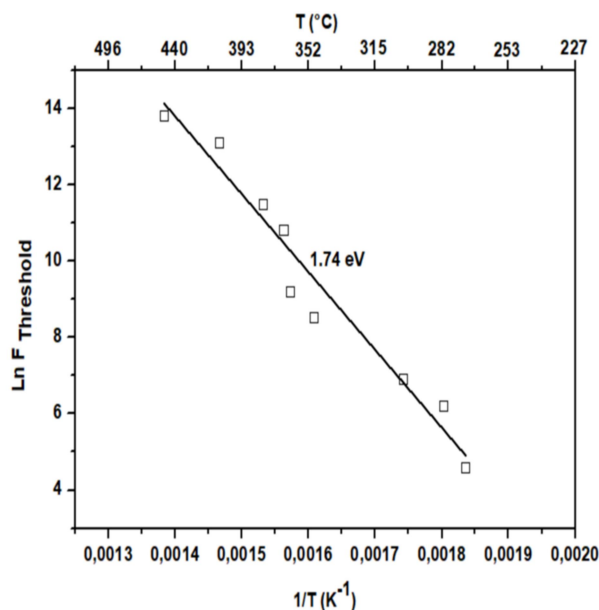


FIG. 6. Threshold frequency (F_T) of the $\text{Sr}_{0.6}\text{Ca}_{0.4}\text{TiO}_3$ ceramic in temperature.

The temperature dependence of the dielectric losses of SCT ceramic from room temperature to 510°C at different frequencies from 100 Hz to 1 MHz (Fig. 7) shows that the dielectric losses remain smaller than 10 up to 200°C from 100 Hz to 1 MHz. The minimum ϵ'' value obtained is 10^{-2} at 10 kHz and 100°C. These low values are very interesting for the development of high-quality factor lead-free ceramic capacitors for applications requiring high temperatures. For frequencies lower than 1 MHz, ϵ'' shows a

minimum around 100°C, which could indicate the existence of dielectric relaxation at low temperatures and low frequencies. Fig. 4 illustrates $\text{tg}\delta$ as a function of frequency. The sharp increase in dielectric losses above about 200°C may be attributed to impurities and thermally activated charge carriers and possible high electrical conductivity at these temperatures in the material [32].

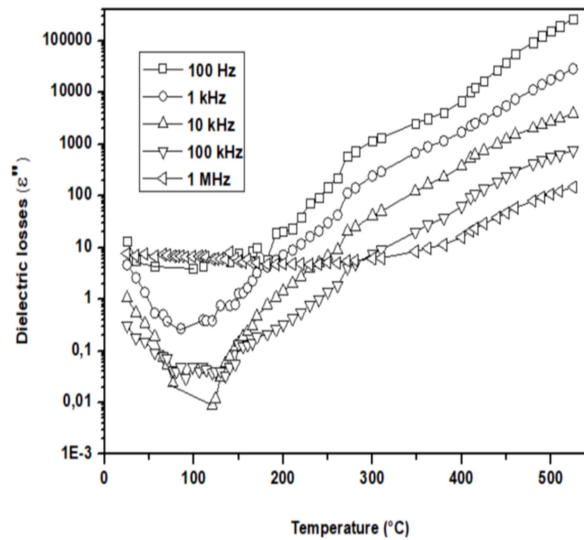


FIG. 7: Dielectric losses (ϵ'') of the $\text{Sr}_{0.6}\text{Ca}_{0.4}\text{TiO}_3$ ceramic in frequency and temperature.

Fig. 8 presents the frequency dependences of dielectric permittivity and dielectric losses at 450°C from 100 Hz to 1 MHz. The dielectric permittivity ϵ' decreases significantly as the measuring frequency increases. This is due to charging mechanisms at the electrodes [33]. Indeed, at low frequencies, ions have enough time to accumulate at the interface of the conductive regions, but at high frequency, they

cannot accumulate at the interface and therefore cannot be polarized. Dielectric losses ϵ'' decrease as the measurement frequency increases, like ϵ' . This frequency effect at high temperature on dielectric losses is attributed to the formation of a space charge region at the electrode-sample interface (contribution on ϵ'), explained in terms of oxygen vacancies diffusion [34].

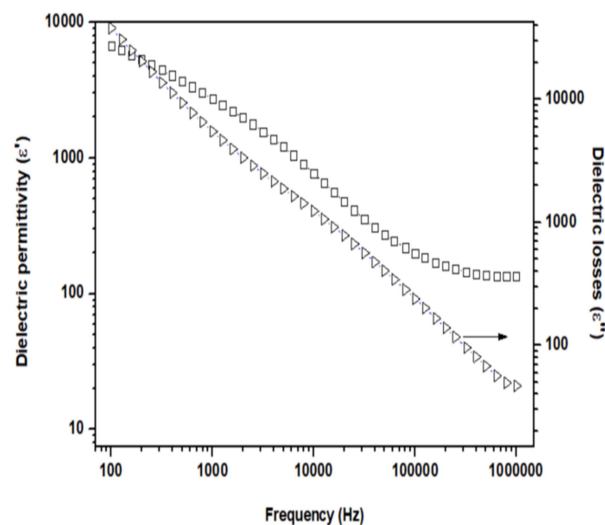


FIG. 8: Dielectric permittivity (ϵ') and dielectric losses (ϵ'') of the $\text{Sr}_{0.6}\text{Ca}_{0.4}\text{TiO}_3$ ceramic in frequency at 450°C.

Electrical conductivity makes it possible to explain the phenomenon of ion transport in the material. The real part of the electrical conductivity σ' of a material is given by the formula: $\sigma' = \omega \cdot \epsilon_0 \cdot \epsilon''$

According to Jonscher, the origin of the evolution of the conductivity as a function of frequency is due to ionic relaxation in the material [35]. The temperature dependence of

the conductivity of the SCT ceramic is shown in Fig. 9, from room temperature to 510°C and at different frequencies from 100 Hz to 1 MHz. At a given frequency, the conductivity has the same temperature-dependent appearance as the dielectric losses (Fig. 7), which shows that the dielectric losses are also due to the electrical conductivity in the material.

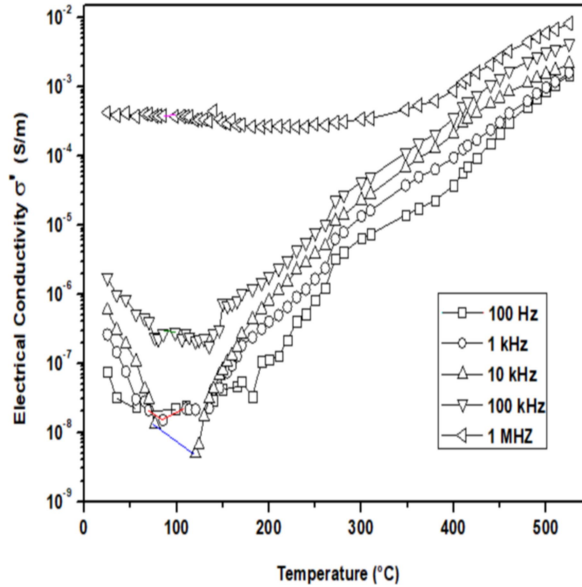


FIG. 9. Conductivity (σ') of the $\text{Sr}_{0.6}\text{Ca}_{0.4}\text{TiO}_3$ ceramic in frequency and temperature.

Fig. 10 shows the Arrhenius plots of $\ln \sigma'$ versus $1/T$ for the ceramic at different frequencies: from 100 Hz to 1 MHz. The conductivity σ' increases strongly with temperature from 127°C for frequencies between 100 Hz and 100 kHz and from 400°C for 1 MHz.

This variation is attributed to the charge carriers hopping due to the high temperature jumping process [36]. At 1 MHz, σ' is constant up to 300°C with a value of about 3×10^{-4} S/m. Above 400°C , the conductivity is thermally activated with the Arrhenius formula (2).

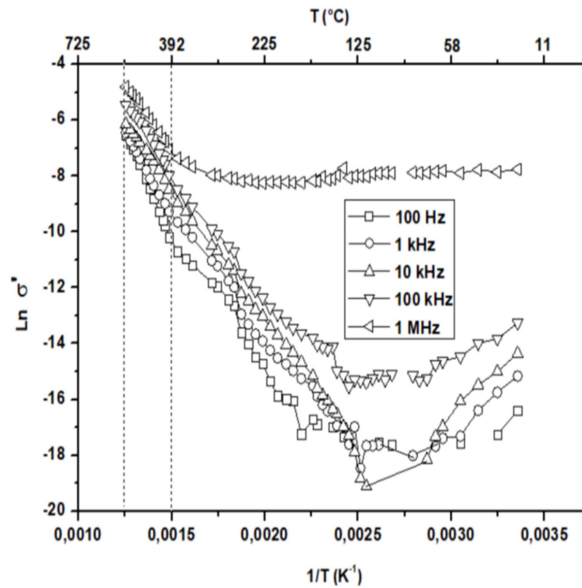


FIG. 10. Conductivity (σ') of the $\text{Sr}_{0.6}\text{Ca}_{0.4}\text{TiO}_3$ ceramic in frequency and temperature.

$$\sigma_{AC} = \sigma_0 e^{\frac{-E_a}{k_B T}} \quad (2)$$

Fig. 11 shows the Arrhenius plots of $\ln \sigma'$ from 400°C to 510°C and at different frequencies from 100 Hz to 1 MHz. The calculated activation energy E_a decreases with the increase of frequency: from 1.38 eV at 100 Hz to 0.86 eV at 5 kHz. For frequencies higher than 5 kHz, the activation energy increases

slightly until 0.93 eV at 100 kHz and then decreases to 0.84 eV at 1 MHz. The activation energy is due to the movement of the charge carriers and to jumps of oxygen vacancies as well as to structural defects at high temperatures [36-37]. The values obtained show that the activation energy is due to the clustering and dissociating processes of the oxygen vacancies [38].

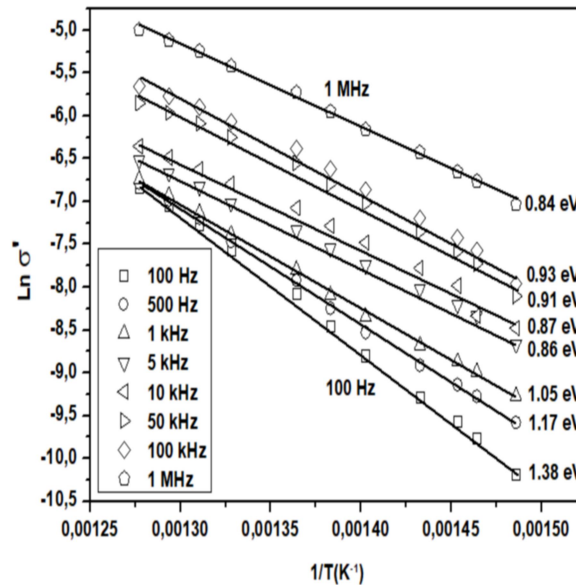


FIG. 11. Arrhenius plots of the conductivity of the $\text{Sr}_{0.6}\text{Ca}_{0.4}\text{TiO}_3$ ceramic from 400°C to 510°C given for frequencies ranging from 100 Hz to 1 MHz.

Fig. 12 shows the frequency dependence from 100 Hz to 1 MHz of the conductivity activation energy E_a . All E_a values have been extracted from Fig. 11, where the temperature ranges from 400°C to 510°C. This curve shows two distinct regions: The first in low frequency from 100 Hz to 5 kHz and the second in medium frequency from 5 kHz to 1 MHz. In the first region, the activation energy decreases significantly with the increase of frequency, while in the second, it increases slightly. The low frequency region could first concern continuous conductivity and then grain boundaries. In fact, at low frequency, the continuous conductivity is sensitive to long-range ion transport usually determined by much higher activation energies [39]. In addition, in grain boundaries, the activation energy is higher

than that in grains due to potential barriers in grain boundaries. The second region could mainly concern oxygen vacancies in the ceramic grains. The activation energy is lower in this region due to short-range ordering of oxygen vacancies [40]. The respective contributions of grains and grain boundaries to the electrical conductivity of the ceramic, at low frequency for grain boundaries and at high frequency for grains, are proven by complex impedance measurement results obtained otherwise [41]. The slight increase in activation energy at high frequency may be due to the creation of charge carriers, such as the formation of doubly-ionized oxygen vacancies [36, 42-47].

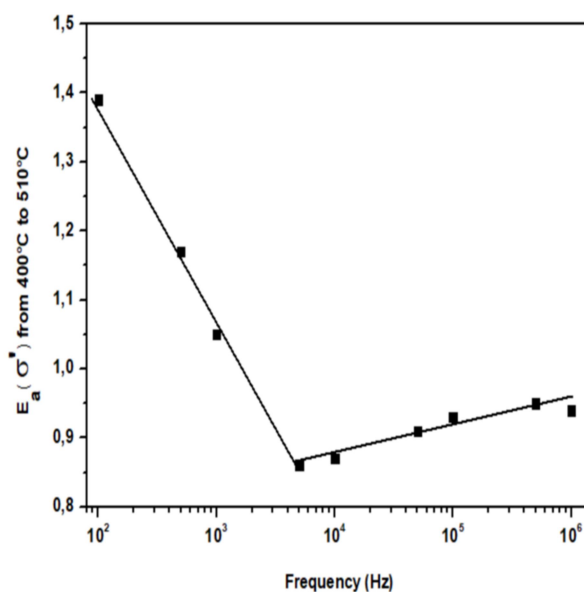


FIG. 12. Conductivity activation energy (E_a) of the Sr_{0.6}Ca_{0.4}TiO₃ ceramic as a function of frequency. All E_a values are related to temperatures ranging from 400 to 510°C.

Conclusion

Sr_{0.6}Ca_{0.4}TiO₃ ceramic was prepared using the solid-state reaction route. XRD analysis revealed an orthorhombic perovskite structure of the material. The ceramic presents homogeneous morphology and dense microstructure. The ceramic exhibits stable dielectric permittivity and low dielectric losses in a wide frequency range from 100 Hz to 1.8 GHz and at temperatures up to 200°C, which shows that the ceramic is a good candidate for the development of monolithic ceramic capacitors dedicated to

high-frequency lead-free components and/or to extremely high-temperature environments. Increasing the temperature beyond 200°C resulted in an increase of the oxygen vacancy concentration and thermally activated charge carriers, which led to an increase of both the dielectric permittivity and dielectric losses. The evolution of the conductivity activation energy as a function of frequency above 400°C can be linked to the existence of two conduction mechanisms in the material.

References

- [1] Outzourhit, A. and Trefny, J.U., *J. Mater. Res. Soc.*, 10 (1995) 1411.
- [2] Jeon, J.H., *J. Eur. Ceram. Soc.*, 24 (2004) 1045.
- [3] Burgnies, L., Vélú, G., Blary, K., Carru, J.-C. and Lippens, D., *Electronic Letters*, 43 (21) (2007) 1151.
- [4] Wu, L., Chen, Y.-C., Chen, L.-J., Chou, Y.-P. and Tsai, Y.-T., *Jpn. J. Appl. Phys.*, 38 (1999) 5612.
- [5] Jacob, M.V., *Int. J. Mod. Phys. B*, 23 (2009) 3649.
- [6] Gonçalves, M.D. et al., *Ceram. Int.*, 42 (2016) 14423.
- [7] Aboubaker, S. et al., *Int. J. Hydrog. Energy*, 42 (2017) 19504.
- [8] Panda, P.K., *J. Mater. Sci.*, 44 (2009) 5049.
- [9] Guo, H., Shimizu, H. and Randall, C.A., *J. Appl. Phys.*, 118 (2015) 174107.
- [10] Puli, V.S. et al., *J. Phys. Chem. Solids*, 74 (2013) 466.
- [11] Cross, L.E., *Mater. Chem. Phys.*, 43 (1996) 108.
- [12] Reymond, V., PhD Thesis, Université de Bordeaux I (2004), France.
- [13] Wang, Z., Cao, M., Song, Z., Li, G., Hu, W., Hao, H. and Liu, H., *Ceram. Int.*, 40 (9) (A) (2014) 14127.

- [14] Xie, J. et al., *Ceram. Int.*, 42 (2016) 12796.
- [15] Wang, R., Inaguma, Y. and Itoh, M., *Mater. Res. Bull.*, 36 (2001) 1693.
- [16] Tkach, A., Vilarinho, P.M. and Kholkin, A., *Appl. Phys. A*, 79 (2004) 2013.
- [17] Ranson, P. et al., *J. Raman Spectrosc.*, 36 (2005) 898.
- [18] Zhanga, L., Yaoa, Z., Lanaganc, M.T., Haoa, H., Xiea, J., Xua, Q., Yuan, M., Sarkarat, M., Caoa, M. and Liua, H., *Journal of the European Ceramic Society*, 38 (2018) 2534.
- [19] Qi, J., Cao, M., Chen, Y., He, Z., Tao, C., Hao, H., Yao, Z. and Liu, H., *Journal of Alloys and Compounds*, 772 (2019) 1105.
- [20] Zhang, L., Hao, H., Zhang, S., Lanagan, M.T., Yao, Z., Xu, Q., Xie, J., Zhou, J., Cao, M. and Liu, H., *Journal of the European Ceramic Society*, 100 (2017) 4638.
- [21] Mishra, S.K., Ranjan, R. and Pandey, D., *J. Appl. Phys.*, 91 (7) (2002) 4447.
- [22] Anwar, S. and Lalla, N.P., *J. Solid State Chem.*, 181 (2008) 997.
- [23] Zhang, G.F. et al., *J. Mater. Sci. Mater. Electron.*, 26 (2015) 2726.
- [24] Ranjan, R. and Pandey, D., *J. Phys.: Condens. Mater.*, 13 (2001) 423.
- [25] Anwar, S. and Lalla, N.P., *Appl. Phys. Lett.*, 92 (2008) 212901.
- [26] Duan, S. et al., *J. Mater. Sci. Mater. Electron.*, 27 (2016) 6318.
- [27] <http://www.ccp14.ac.uk/tutorial/lmgp/celref.htm>
- [28] Tagantsev, A.K., Sherman, V.O., Astafiev, K.F., Venkatesh, J. and Setter, N., *Journal of Electroceramics*, 11 (2003) 5.
- [29] Ait Laasri, H., Fasquelle, D., Tachafine, A., Tentillier, N., Costa, L.C., Elaati, M., Outzourhit, A. and Carru J.-C., *Functional Materials Letters*, 11 (5) (2018) 1850005.
- [30] Maxwell, J., "A Treatise on Electricity and Magnetism". (Cambridge University Press, 1873).
- [31] Ang, C. and Yu, Z., *Phys. Rev. B*, 62 (2000) 228.
- [32] Sahoo, S., Mahapatra, P.K., Choudhary, R.N.P. and Nandagoswamy, M.L., *J. Mater. Sci.: Mater. Electron.*, 26 (2015) 6572.
- [33] Om, P.N. et al., *Indian. J. Pure Appl. Phys.*, 48 (2010) 57.
- [34] Mariappan, C.R. and Govindaraj, G., *Mater. Sci. Eng., B.*, 94 (2002) 82.
- [35] Dhak, P., Dhak, D., Das, M. and Pramanik, P., *J. Mater. Sci.: Mater. Electron.*, 22 (2011) 1750.
- [36] Liu, L., Huang, Y., Su, C., Fang, L., Wu, M., Hu, C. and Fan, H., *Appl. Phys. A*, 104 (2011) 1047.
- [37] Rout, J., Parida, B.N., Das, P.R. and Choudhary, R.N.P., *J. Electron. Mater.*, 43 (2014) 732.
- [38] Wang, C.C., Lei, C.M., Wang, G.J., Sun, X.H., Li, T., Huang, S.G., Wang, H. and Li, Y.D., *J. Appl. Phys.*, 113 (2013) 094103.
- [39] Dunst, A., Epp, V., Hanzu, I., Freunberger, S.A. and Wilkening, M., *Energy Environ. Sci.*, 7 (2014) 2739.
- [40] McCammon, C.A., Becerro, A.I., Langenhorst, F., Angel, R.J., Marion, S. and Seifert, S., *J. Phys.: Condens. Matter*, 12 (2000) 2969.
- [41] Tachafine, A., Ait Laasri, H., Carru, J.C. and Fasquelle, D., to be published.
- [42] Verdier, C., Morrison, F.D., Lupascu, D.C. and Scott, J.F., *J. Appl. Phys.*, 97 (2005) 024107.
- [43] Yoo, H.I., Song, C.R. and Lee, D.K., *J. Electroceram.*, 8 (2002) 5.
- [44] Smyth, D.M., *J. Electroceram.*, 11 (2003) 89.
- [45] Moos, R., Menesklou, W. and Härdtl, K.H., *Appl. Phys. A*, 61 (1995) 389.
- [46] Moos, R. and Härdtl, K.H., *J. Appl. Phys.*, 80 (1996) 393.
- [47] Maglione, M. and Belkaoui, M., *Phys. Rev. B*, 45 (1992) 202.